NeuroImage: Clinical 20 (2018) 61–70

Contents lists available at ScienceDirect

NeuroImage: Clinical

journal homepage: www.elsevier.com/locate/ynicl

# Multi-component relaxation in clinically isolated syndrome: Lesion myelination may predict multiple sclerosis conversion

Hagen H. Kitzler[a,*,1], Hannes Wahl[a,1], Judith C. Eisele[b], Matthias Kuhn[c], Henning Schmitz-Peiffer[b], Simone Kern[b], Brian K. Rutt[d], Sean C.L. Deoni[e], Tjalf Ziemssen[b], Jennifer Linn[a]

[a] Dept. of Neuroradiology, Technische Universität Dresden, Dresden, Germany
[b] Dept. of Neurology, Technische Universität Dresden, Dresden, Germany
[c] Institute of Medical Informatics and Biometry, Technische Universität Dresden, Dresden, Germany
[d] Richard M. Lucas Center for Imaging, School of Medicine, Department of Radiology, Stanford University, Stanford, CA, USA
[e] Memorial Hospital of Rhode Island, Warren Alpert Medical School, Brown University, Providence, RI, USA

ARTICLE INFO

*Keywords:*
Clinically isolated syndrome
Multiple sclerosis
Myelin imaging
MRI
Multicomponent relaxation
mcDESPOT

ABSTRACT

We performed a longitudinal case-control study on patients with clinically isolated syndrome (CIS) with the aid of quantitative whole-brain myelin imaging. The aim was (1) to parse early myelin decay and to break down its distribution pattern, and (2) to identify an imaging biomarker of the conversion into clinically definite Multiple Sclerosis (MS) based on *in vivo* measurable changes of myelination.

Imaging and clinical data were collected immediately after the onset of first neurological symptoms and follow-up explorations were performed after 3, 6, and, 12 months. The *multi-component Driven Equilibrium Single Pulse Observation of T1/T2* (mcDESPOT) was applied to obtain the volume fraction of myelin water (MWF) in different white matter (WM) regions at every time-point. This measure was subjected to further voxel-based analysis with the aid of a comparison of the normal distribution of myelination measures with an age and sex matched healthy control group. Both global and focal relative myelination content measures were retrieved.

We found that (1) CIS patients at the first clinical episode suggestive of MS can be discriminated from healthy control WM conditions ($p < 0.001$) and therewith reproduced our earlier findings in late CIS, (2) that deficient myelination in the CIS group increased in T2 lesion depending on the presence of gadolinium enhancement ($p < 0.05$), and (3) that independently the CIS T2 lesion relative myelin content provided a risk estimate of the conversion to clinically definite MS (*Odds Ratio 2.52*).

We initially hypothesized that normal appearing WM myelin loss may determine the severity of early disease and the subsequent risk of clinically definite MS development. However, in contrast we found that WM lesion myelin loss was pivotal for MS conversion. Regional myelination measures may thus play an important role in future clinical risk stratification.

## 1. Introduction

### 1.1. Clinically isolated syndrome

The clinically isolated syndrome (CIS) is a condition defined as a > 24 h lasting episode of sudden performance restriction in neuronal systems that occurs at one or more functional areas of the central nervous system (CNS) (Krupp et al., 2007, 2013; Miller et al., 2005a). Caused by an acute inflammatory demyelinating event, approximately 85% of all patients that subsequently develop multiple sclerosis (MS) exhibit this initial clinical presentation (Miller et al., 2008). In many CIS patients conventional magnetic resonance imaging (MRI) reveals

*Abbreviations:* EDSS, extended disability status scale; DAWM, diffusely abnormal white matter; DVF, deficient volume fraction of myelin water; FLASH, fast low-angle shot; mcDESPOT, multi-component Driven Equilibrium Single Pulse Observation of T1/T2; MCRI, multicomponent relaxation imaging; MSFC, multiple sclerosis functional composite; MWF, myelin water fraction; NAWM, normal appearing white matter; trueFISP, true fast imaging with steady state precession

* Corresponding author at: Institut und Poliklinik für Diagnostische und Interventionelle Neuroradiologie, Universitätsklinikum Carl Gustav Carus, Technischen Universität Dresden, Fetscherstrasse 74, 01307 Dresden, Germany.
*E-mail address:* Hagen.Kitzler@uniklinikum-dresden.de (H.H. Kitzler).
[1] Equally contributed to this work.

https://doi.org/10.1016/j.nicl.2018.05.034
Received 24 January 2018; Received in revised form 1 May 2018; Accepted 27 May 2018
Available online 31 May 2018

multifocal white matter (WM) lesions that complement the diagnostically relevant spatial or temporal dissemination and thereby allow the diagnosis of MS based on the 2010 revised McDonald criteria (Polman et al., 2011).

The relationship between conventional brain MRI features and the short-term risk of CIS patients developing definite MS has been assessed by several studies. *Korteweg and colleagues* collaboratively studied a large cohort of patients with CIS focusing on WM lesions and the evidence for dissemination in space. They found a conversion rate of 45%, with a more than four times increased relative risk of conversion in patients with an abnormal MRI versus patients with no initial WM lesions (10%), after 2 years follow-up (Korteweg et al., 2007). Further CIS cohort studies spanning 7 through 20 years of follow-up investigated the long-term risk of MS development and found conversion rates of 65–80% for patients with an abnormal conventional MRI and 8–20% for those with an inconspicuous baseline MRI (Tintore et al., 2006; Fisniku et al., 2008). However, in CIS patients with initial multifocal clinical symptom presentation the abnormal MRI did not stratify the risk for clinically definite disease conversion (Nielsen et al., 2009).

The limited predictive value of conventional MRI disease surrogates in CIS and early MS is assumed to originate both from a limited sensitivity for subtle non-lesional tissue changes and from a severely limited specificity for pathologic substrates. It is known, for example, that demyelination, one of the hallmarks of MS neuropathology, is not directly depicted by conventional MRI (Cicarelli, 2000). On the contrary, a variety of quantitative MRI techniques have found subtle abnormalities beyond WM lesions in otherwise normal appearing brain tissue (see overview by (Miller et al., 2005b)). We were therefore motivated in this study to apply quantitative myelin imaging in a population of CIS patients and matched controls, testing its value for predicting MS conversion.

### 1.2. Myelin imaging

#### 1.2.1. Multicomponent relaxation

Magnetic resonance myelin imaging using multicomponent relaxation imaging (MCRI) has become a valuable tool for exploring tissue-specific differences in demyelinating disorders. Early work in MS was based on multi-echo spin-echo measurements which were then subjected to multi-component T2 analysis (T2-MCRI), allowing the water signal of WM to be separated into three components: (1) a long T2 component (~2 s) derived from cerebrospinal fluid, (2) an intermediate component (~100 ms) arising from intracellular and extracellular water, and (3) a short T2 component (~20 ms) originating from water trapped between the myelin bilayers, the so-called myelin water (Whittall et al., 1997). The relative volume fraction for myelin water for each voxel was termed *myelin water fraction* (MWF) (Laule et al., 2007). This term was adopted by other MRI techniques of myelin water measurement.

#### 1.2.2. mcDESPOT

To overcome T2-MCRI restrictions in brain coverage and acquisition speed for clinical research, alternative techniques have been developed to provide rapid and comprehensive CNS coverage. The most promising alternative to the established T2-multiecho approach is the *multi-component driven equilibrium single pulse observation of T1 and T2* (mcDESPOT). Although the correspondence is subject to ongoing research the MWF derived from mcDESPOT most closely resembles T2-MCRI derived MWF with strong correlations between values in WM, including in MS and postmortem tissue and reveals a distribution peaked around 0.23 within adult healthy control WM (Kitzler et al., 2012).

We found earlier that normalized myelin water content from MS T2 lesions through WM not affected by lesions distinguished CIS patients from healthy controls. In this precedent single time point study we compared regional MWF in relapsing-remitting, secondary and primary progressive MS patients with CIS. We introduced the voxel-based measure of deficient MWF volume fraction (DVF) derived from WM regions by dividing by the corresponding region volume. Measured in normal appearing WM this quantity discriminated CIS patients from healthy controls and discriminated relapsing–remitting from secondary-progressive patients. We concluded that this measure may sense early disease-related myelin loss and important transitions from CIS to definite and further progressive disease (Kitzler et al., 2012).

For this present study we hypothesize that myelin measures in CIS would predict the conversion to MS and thus define CIS patients at risk for definite disease development. However, within our initial comparison of different MS courses, the CIS sub-cohort was recruited without attention to the interval between initial diagnosis and MRI (Kitzler et al., 2012). Since this may have introduced a significant bias in terms of testing the correlation between myelin water measures and disease development, we designed the present study with attention to this time interval, and with the following goals: (1) to reproduce the important finding of very early myelin loss in CIS and (2) to study the predictive ability of various myelin water measures in relation to MS conversion.

## 2. Materials and methods

### 2.1. Recruitment and data acquisition

A total of sixteen individuals classified as CIS were recruited immediately after diagnosis. The local Medical Ethics Review Committee of the Dresden University Hospital approved the recruitment plan and the study protocol. All patients and healthy controls provided written informed consent. Two patients were lost due to drop out after the initial MRI. The median age of the remaining group (n = 14) was 32 years with a male/female ratio of 6/8. Ten patients converted to clinically definite MS before the end of the study period. Six patients started disease-modifying treatment with Copaxone during the study. The healthy control group of 21 subjects had a median age of 31 years and a male/female ratio of 7/14 (see Table 1 for further details of both groups).

All patients underwent clinical disability assessment and the *extended disability status scale* (EDSS; (Kurtzke, 1983)) score was determined at baseline and after 12 months. In addition the *multiple sclerosis functional composite* (MSFC; (Cutter et al., 1999)) was measured at four time-points on the same day as the MRI data acquisition (see Table 3). The conversion of CIS to clinically definite MS was defined by either a subsequent clinical relapse or the appearance of new WM lesions fulfilling both temporal and spatial disease dissemination based on current diagnostic criteria (Polman et al., 2011).

### 2.2. MRI acquisition and processing

A 1.5 Tesla MR scanner (*Siemens Magnetom Sonata, Siemens Healthcare, Erlangen, Germany*) equipped with an 8-channel radio frequency head coil was used to derive multi-component T1 and T2 information from sets of *fast low-angle shot* (FLASH) and *true fast imaging*

**Table 1**
Demographic and clinical statistics for all patients and healthy controls.

| | CIS subjects (n = 16) | Healthy controls (n = 21) |
|---|---|---|
| Male/female | 6/10 | 7/14 |
| Conversion | 10/16 | – |
| Age (*years*) | *Min … Max/Median* (IQR) | *Min … Max/Median* (IQR) |
| | 22.0 … 50.0 | 23.0 … 44.0 |
| | 32.0 (11.0) | 31.0 (10.0) |
| Days since symptoms onset | 16.0 … 207.0 | – |
| | 71.0 (62.0) | |

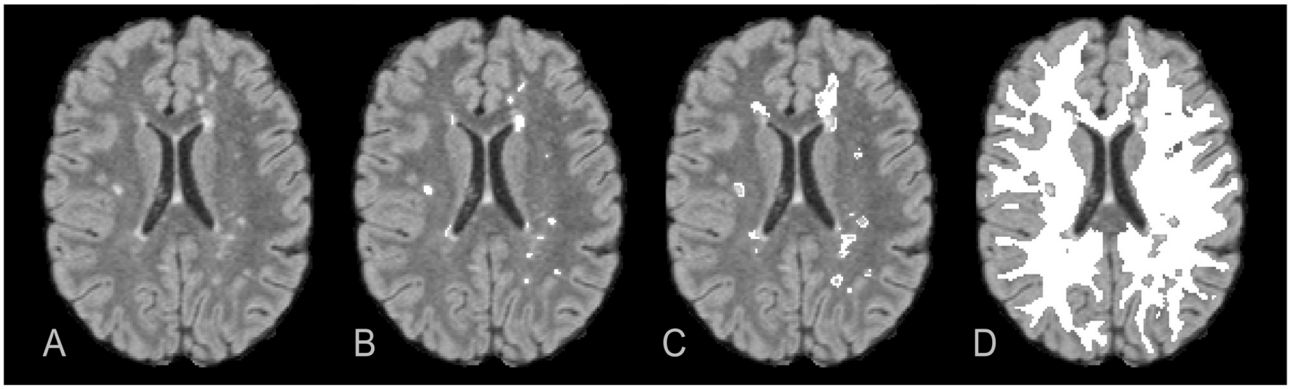


**Fig. 1.** WM tissue segmentation separately marked in 3D-FLAIR axial reformat (A). Multiple T2-hyperintense lesions were selected by semi-automated segmentation and manually edited (B). DAWM tissue volumes characterized by intermediate T2 signal were retrieved by selectively applying an increased threshold around T2 lesion (C). Finally the subtraction of T2 lesion and DAWM volume from total WM segmentation resulted into NAWM (D). All regions were 3D-resolved binary maps.

*with steady state precession* (trueFISP) data acquired over a range of flip angles at constant echo time (TE) and repetition time (TR) using the following specifications: field of view (FOV) = 22 cm, image matrix = 128 × 128, slice thickness = 1.7 mm; FLASH: TE/TR = 2.0/5.7 ms, flip angle (α) = [5, 6, 7, 8, 9, 11, 13, 18]°; trueFISP: TE/TR = 1.71/3.42 ms, α = [9, 14, 19, 24, 28, 34, 41, 51, 60]°. Since the B1 inhomogeneity is very small for 1.5 T it was neglected. The total mcDESPOT acquisition time (TA) was ~13 min. A T1 weighted anatomical reference scan (2D-T1 spin echo: TE/TR = 12/500 ms, FOV = 22 cm, matrix = 256 × 256, slice thickness = 3 mm, TA = 6:30 min) and a 3D spatially resolved *fluid-attenuated inversion recovery* (3D-FLAIR) sequence (TE/TR = 353/6000 ms, TI = 2200 ms, FOV = 22 × 22 cm, image matrix = 256 × 210, slice thickness = 1 mm, TA = 5:50 min) with whole-brain coverage to identify lesions were acquired.

### 2.3. MRI data processing

#### 2.3.1. Multicomponent relaxation data processing

Data post-processing was executed by sets of python scripts to automate the *FMRIB Software Library* (FSL). First brain extraction was performed (Jenkinson et al., 2005), followed by an intra-subject linear co-registration using FLIRT (Smith, 2002) with 12° of freedom to a selected target (SPGR image α = 18°) and down sampling to a 160 × 160 × 96 resolution to reduce processing time and achieve isotropic voxel size. The registered series were fitted to the mcDESPOT algorithm to estimate the two-compartment model parameters of tissue water distribution for 1.5 T data (Deoni et al., 2008). The MWF maps of both patients and healthy controls were non-linearly registered to the MNI152 1 $mm^3$ isotropic resolution standard brain space (*International Consortium for Brain Mapping standard template*) using the FSL v5.0 tools FLIRT and FNIRT (Jenkinson and Smith, 2001; Jenkinson et al., 2002; Greve and Fischl, 2009). FLIRT with 12° of freedom yielded the initial affine guess for FNIRT, which was run with the predefined configuration "*T1_2_MNI152_2mm.cnf*" provided by FSL and a warp resolution of 8, 8, 8 mm for every stage. The resulting warps were then used with the 1 mm^3 isotropic template. Subsequently $z$-scores were calculated based on the MWF healthy control data value distribution (Kitzler et al., 2012).

The resulting $z$-score maps were re-warped into the native subject space and a threshold of $z \leq -4$ ($p < 0.00003$) was applied to discriminate deficient MWF voxels. The same very conservative threshold was used as in our previous study to allow quantification of differences with sufficient specificity with respect to short-term MWF changes. Those deficient MWF voxels were added up to the *deficient MWF volume* (DV) for each tissue region (see next sub-section for further details). Finally dividing DV by the respective region volume produced the *deficient* MWF *volume fraction* (DVF) as an inter-subject comparative computation of normalized myelin deficiency for each tissue region.

#### 2.3.2. Brain matter region segmentation and volume estimation

Conventional MRI data were used to segment brain tissue regions and WM pathology. By means of the *Statistical Parametric Mapping* software package (SPM8; *Wellcome Department of Imaging Neuroscience*, UCL, London, UK) T1-weighted SE data was segmented into grey matter (GM) and WM (Ashburner and Friston, 2005). The resulting probability maps were converted into binary masks by applying a threshold of 0.5 and a median filter with a 3 × 3 × 3 voxel kernel to reduce noise-related errors. An experienced radiologist (*HHK*) edited the resulting WM masks. Voxels below the pons level were excluded in order to standardize the analyzed brain parenchyma. Manual adjustment was further applied to exclude false positively segmented areas based on neuroanatomical considerations. Special care was taken to fill in lesions in WM masks and to eliminate areas in the proximity of ventricular cerebrospinal fluid (CSF) spaces and GM to avoid partial volume effects. Registering every subsequent time-point of T1, FLAIR and mcDESPOT data to the baseline T1 scan enabled efficient longitudinal analysis and reduced additional tissue mask editing bias.

*T2 lesions* (T2L) were identified as well-defined focal areas of elevated T2 signal intensity in FLAIR data. Semi-automatic segmentation was applied by using $z$-score thresholding of $z > 4$ against normalized FLAIR intensity with preceding normalization by a *robust maximum* (98%) (Kitzler et al., 2012). The resulting maps were manually edited using the ITK-Snap software package (Yushkevich et al., 2006) (see Fig. 1B).

*Diffusely abnormal white matter* (DAWM) regions, defined as areas of intermediate T2 signal intensity between focal lesions and WM (Fazekas et al., 1999) were segmented by thresholding the edited T2L maps at $z > 2$. Every 3D region of the resulting masks without intersection to a previously defined T2L segmentation was discarded with the aid of MATLAB (Kitzler et al., 2012). The DAWM mask was generated by finally subtracting the T2L segmentation from the latter result (see Fig. 1C).

At last, the *normal appearing white matter* (NAWM) tissue mask was calculated by subtracting both diffusely abnormal WM and T2 lesion segmentation results from the overall segmented WM ($NAWM = WM - DAWM - T2L$) (see Fig. 1D).

Mean MWF values and the normalized DVF measures were determined for every individual total WM and the segmented WM regions in patients and the WM of the healthy controls. The segmented WM regions of the baseline acquisition were transmitted to the subsequent time points for tissue-specific longitudinal observation.

Complementary brain matter volume estimation was done using SIENAX as part of FSL (Smith et al., 2004) to avoid rater bias in the

segmentation and to ensure consistency in volume estimation. After brain extraction and affine registration to the MNI152 space (see Section 2.3.1) the achieved volumetric scaling factor was applied as normalization for individual head size. Finally the total brain parenchyma volume and volume estimates of WM, central and peripheral GM and CSF were retrieved by tissue-type segmentation with partial volume estimation (Zhang et al., 2001).

### 2.4. Statistical methods

For two-group comparison the non-parametric *Mann-Whitney U test* was used. Time course data were analyzed using linear mixed models where random effects adjust for the repeated measures on subject and brain region level. We adjusted *p*-values for multiple comparisons at different time points within a brain sub-region. Correlations between repeated measures (*like between DVF and MSFC*) were estimated via a generalized least squares regression model that corrects for mean changes over time and that allows for separate variance for each variable. Univariate prediction models relating to the MS-conversion status were built by means of an optimal cutoff that yielded best sensitivity and specificity (*Youden Index*). The performances of these classifiers were assessed via *receiver-operating characteristic* (ROC) curves and their *area under the curve* (AUC), which measures the predictor's ability to discriminate between the two MS-conversion states. To avoid overfitting, the AUC values were calculated using regular bootstrap, i.e. the respective classifier was repeatedly (B = 1500 bootstrap samples) built on the data set after re-sampling with replacement and evaluated on the remaining cases that were not re-sampled.

We analyzed the variation of repeated myelin measures within subjects per brain region. The applied linear mixed model portioned the total variance of observations into intra-subject variance and between-subject variance after adjusting for fixed time effects. Further, the intra-class correlation coefficient (ICC), i.e. the between-subject variance relative to the total variance was used to estimate the correlation of repeated measurements in a brain region of the same subject (see Section 3.1.3).

All statistical calculations were performed utilizing R 3.4.1.

## 3. Results

### 3.1. White matter myelination assessment

#### 3.1.1. Total white matter measurements in CIS and healthy controls

The median total WM MWF demonstrated no significant difference between CIS patients and healthy controls. In contrast the median DVF was significantly increased in CIS patients compared to healthy controls (0.3977% vs. 0.0023%; *Mann-Whitney U test with continuity correction*, $p < 0.001$, see Fig. 2).

#### 3.1.2. Regional white matter myelination measurements

Remarkable differences in MWF and DVF were observed between the NAWM, DAWM and T2L regions for both MWF and DVF (Table 2 and Fig. 3). Whereas NAWM featured high MWF measurements in combination with low values of DVF, i.e. low deficient myelination rate, the opposite was the case in the DAWM and in particular in the T2L region. According to our linear mixed model, mean MWF across the study period was 0.231 (95%-CI: 0.222–0.239) in NAWM, 0.213 (95%-CI: 0.204–0.222) in DAWM and 0.148 (95%-CI: 0.139–0.158) in T2L. Mean DVF showed the opposite pattern with 0.670% (95%-CI: 0–6.311%) in NAWM, 8.574% (95%-CI: 2.800–14.348%) in DAWM and 20.522% (95%-CI: 14.756–26.289%) in T2L. Aware of the fact that the normalized DVF might be influenced by early brain tissue volume loss (atrophy) we controlled the studied cohort for this feature. Using the *Mann-Whitney-U test* no differences were found for volumes of WM and GM tissue between healthy controls and CIS patients neither at baseline nor after 12 months (*not graphically displayed here*).

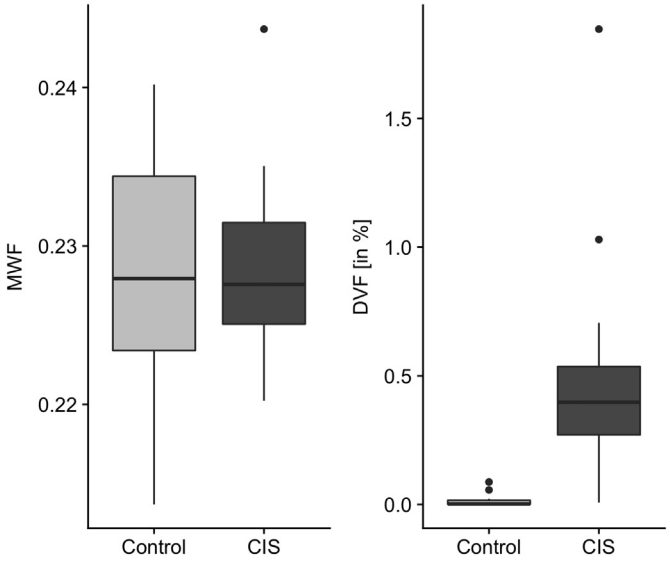


**Fig. 2.** Comparative plots of both median MWF and DVF for total WM in healthy controls and the CIS group at baseline showing a significant difference in normalized deficient myelination measures (DVF) between the two groups.

Compared to healthy control WM at baseline, CIS patients showed at all time points a significant MWF decrease in the DAWM and T2L compartments, and a significant DVF increase in all regions NAWM, DAWM and T2L (*Mann-Whitney U test,* see Table 2).

#### 3.1.3. Longitudinal regional myelination observations

We investigated the longitudinal change of myelin measures in the CIS patients within the 12-month study period at four time points (see Fig. 3). According to the applied linear mixed model, there was no time point that showed a significant mean change in MWF at any specific tissue region. With respect to DVF, we observed a significant mean increase at the last time point in NAWM. In T2L interestingly, the last two time points showed significant lower mean DVF values compared to the first two time points.

The repeated myelin measures showed a strong correlation within the measurement regions and within the individual subjects over time. Of these regions, NAWM revealed the smallest residual variability in the data, both for MWF and for DVF (see Table 3). However, the inter-patient variability outweighed the longitudinal intra-patient variability in both MWF and DVF measurements. The residual variability in DAWM and in T2L was significantly increased compared to the NAWM sub-region, for both MWF ($p = 0.0008$) and for DVF ($p < 0.0001$).

Healthy controls in comparison had an inter-subject variance of 0.008 and 0.022, for MWF and DVF, respectively. The MWF variance of their healthy WM was comparable to patient MWF variability in NAWM, while the DVF measures showed a much higher variability in patients (see Table 3).

### 3.2. Myelination and outcome measures

The median baseline EDSS of 1.5 remained unchanged at one year follow up (*Wilcoxon signed rank test;* $p = 0.389$). The mean MSFC score revealed a minor but continuing increase of 0.23 per 12 months ($p = 0.0015$) during the study period. Both clinical scores were negatively correlated across time ($r = -0.47$, $p = 0.013$) (see Table 4) in accordance with their opposite orientation.

The estimated correlations between EDSS and MSFC and respective MWF and DVF within the pathologic WM regions of patients were evaluated and revealed the strongest correlation between DVF in DAWM with MSFC ($r = 0.314$, $p = 0.022$) and inversely the EDSS ($r = -0.484$, $p = 0.006$) again in counter-intuitive direction.

**Table 2**
MWF and DVF in pathologically defined WM sub-regions at baseline and of follow-up scans in CIS patients. For each time point and each sub-region, we compared the CIS-patients against the healthy control group at baseline with Mann-Whitney's U test. Significance levels are marked with * $p < 0.05$ and ** $p < 0.001$.

| Region | Baseline (n = 16) | | 3 months (n = 14) | | 6 months (n = 13) | | 12 months (n = 14) | |
|---|---|---|---|---|---|---|---|---|
| | MWF | DVF [%] | MWF | DVF [%] | MWF | DVF [%] | MWF | DVF [%] |
| | Mean (STD) | | Mean (STD) | | Mean (STD) | | Mean (STD) | |
| NAWM | 0.229 (0.006) | 0.5* (0.4) | 0.230 (0.006) | 0.6* (0.8) | 0.233 (0.008) | 0.4* (0.5) | 0.230 (0.008) | 0.9* (1.0) |
| DAWM | 0.212* (0.022) | 8.9* (9.6) | 0.213* (0.025) | 8.8* (10.9) | 0.218* (0.022) | 6.3* (8.5) | 0.211* (0.022) | 9.4* (10.2) |
| T2L | 0.145** (0.022) | 22.0** (17.7) | 0.148** (0.025) | 23.2** (16.0) | 0.155** (0.026) | 19.7** (18.0) | 0.147** (0.023) | 21.1** (16.9) |

### 3.3. Myelination and inflammatory activity

Regional myelination measurements were subsequently tested for their association with conventional MRI characteristics of inflammatory activity by dichotomizing the patient group at each time point into those of present or absent *blood-brain-barrier* (BBB) disruption, i.e. focal Gadolinium enhancing WM lesions (Fig. 4).

Using a linear mixed model, we estimated the effect of proportion of inflammatory MRI activity (gadolinium enhancement) on MWF and DVF. Changing a patient from never inflammatory active to always inflammatory active was associated on average with a non-significant decrease by 0.022 in MWF in WM lesions (T2L) ($p = 0.1278$), while DVF significantly increased by 26.86 in T2L ($p = 0.0054$). All other region did not reveal significant effects.

### 3.4. Myelination and MS conversion

We dichotomized the CIS patient group retrospectively into those that converted into clinically definite MS based on current clinical diagnostic criteria at 9 months follow-up (*10 out of 16*).

The patient subgroup that converted to MS revealed a reduced mean MWF by 0.018 ($p = 0.051$) and a significantly elevated mean DVF by 18.354 ($p = 0.002$) within WM lesions (T2L; *linear mixed model with conversion status as so-called between-subject factor*) from baseline through the end of the study period (see Fig. 5).

In CIS patients, neither total GM nor total WM volume measurement revealed significant changes across time-points during 12 months follow-up. Total GM or WM volume changes did also not distinguish the MS converters from non-converters (see Table 5).

While MS converters revealed a higher median T2 lesion load ($p = 0.0048$) hardly any effect of T2 lesion load on MWF measures was noted. However, in the T2L region, we estimated a significant average increase of 3.341% in DVF when the T2 lesion load was increased by 10 lesions.

### 3.5. Predicting MS conversion by means of baseline myelination

We explored different baseline variables as classifiers to discriminate subjects achieving the condition of clinically definite MS. The ideal case would allow predicting MS-conversion by a clear decision rule based on short-term preceding and only few measurements. We therefore estimated optimal cutoff values (*Youden Index*) for each baseline predictor and assessed its discrimination ability via its bootstrapped AUC value.

In any WM region of CIS patients, lower values of MWF and higher values of DVF were associated with a higher incidence of conversion to definite MS. However, the best performing baseline variables were (1) MWF in T2L, (2) DVF in T2L and (3) conventional WM T2 lesion load. The relationship of these MRI measures and the incidence of conversion to definite MS are given as conditional density plots in Fig. 6. Since MWF and DVF represent antidromic values both plots illustrate the following relationships: The lower the T2L mean MWF, the higher the risk to convert, and, the higher the T2L DVF the higher the risk to convert. In addition, the higher the T2L load the higher the risk to convert.

As cutoffs of these baseline variables we found MWF = 0.15 in T2L with *odds ratio* (OR) = 2.52, DVF = 13.96% in T2L ($OR = 6.65$) and WM T2 lesion number = 19 ($OR = 3.32$). The corresponding bootstrapped AUC values were 0.70 for MWF in T2L, 0.91 for DVF in T2L and 0.78 for lesion load.

## 4. Discussion

In this study the voxel-based myelination measure DVF and its related mean MWF in CIS patient WM lesions were found promising risk factors for the development of clinical definite MS. An earlier single time-point observation already found DVF and MWF to be significantly different in both WM lesions and NAWM in CIS patients compared to healthy controls (Kitzler et al., 2012). Hereby the discrimination of CIS from healthy controls was confirmed within the first 12 months since symptom onset. In extension of our previous study the main intention was to follow early regional myelin deficiency in CIS. The proposed analysis pipeline was therefore extended to a longitudinal analysis.

Regarding the development of clinical MS, our analysis first reproduced the known relationship that the *higher* the WM lesion load in CIS (Kuhle et al., 2015), the higher the risk to convert to definite MS. Long-term follow-up studies revealed the importance of the burden of T2 lesions at CIS diagnosis for the subsequent MS course and clinical development (Fisniku et al., 2008). However, such conventional MRI measures did not provide short-term risk assessments for those to convert from CIS to MS.

### 4.1. White matter lesion myelination increased the CIS short-term risk to convert to MS

We found that the *lower* the mean MWF, and the *higher* the DVF in WM lesions, the higher the short-term risk to convert to MS. Given the known predominant inflammatory demyelination in CIS and early MS (Charil and Filippi, 2007), the finding that myelin deficiency determines the risk of conversion to definite disease did not come by surprise. However, the significance of focal myelin loss being higher than that of other WM areas is in that sense remarkable since it is even higher than the impact of subtle NAWM myelin loss. This may support the comprehension of MS initiation as an in vivo observable multifocal but confined inflammatory demyelinating process.

We found AUC close to 1 for the prediction model that used DVF in WM lesions, implying that discrimination between converters and non-converters was possible, at least in this training sample. A limitation of our analysis was the estimation of the optimal cutoff value, since precise cutoff estimation usually requires a large patient number and a more robust performance estimation remains to be done in a greater patient cohort.

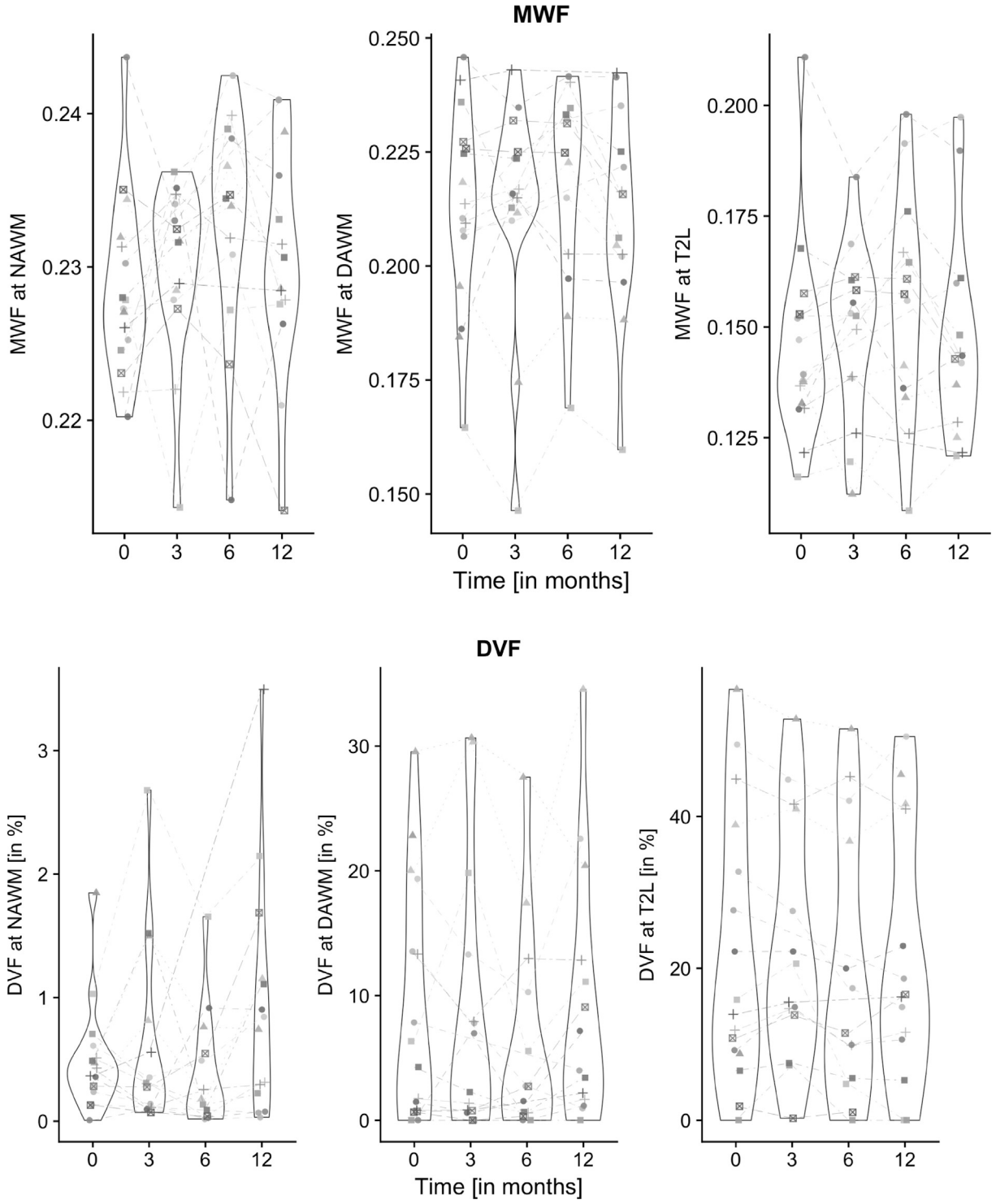


**Fig. 3.** Longitudinal changes of both MWF and DVF of all CIS-patients within the segmented WM sub-regions within the 12 months follow-up. The median and interquartile range (IQR) was plotted for the respective four time points and regions.

### *4.2. Different degrees of individual myelin deficiency found in WM lesions in early MS*

In WM lesions and DAWM the variability of MWF and its normalized DVF within an individual patient (*intra-patient variability* over the study period) was minor compared to the variability between patients (*inter-patient variability*) (see Table 3). This implied a relatively stable measure development over the study period within these WM regions. However, there were wide measurement differences between patients especially of DVF in WM lesions indicating different degrees of individual myelin damage in early MS lesion pathology.

In contrast in NAWM the MWF and DVF the measure variation over time clearly exceeded the variability between patients. This indicated different degrees of demyelination and remyelination in CIS and early MS in NAWM with no detectable lesions by conventional MRI. Assuming progressive break-up of myelinated axons emanating from within initiating lesions the demyelination in WM areas distant to the inflammatory primers may principally succeed the focal myelin loss.

**Table 3**
Intra-patient and inter-patient variance as standard deviation after adjusting for time and brain region effects. The intra-class correlation coefficient (ICC) was determined as the correlation of two measurements of the same patient and the same measurement region after correcting for time effects. Note the smallest ICC in NAWM measures representing the highest variability in individual patient NAWM relative to group variability.

| Measure | Region | Intra-subject variance as $\sigma_{within}$ | Inter-subject variance as $\sigma_{betw}$ | Total variance as $\sigma_{total}$ | ICC |
|---|---|---|---|---|---|
| MWF | NAWM | 0.005 | 0.004 | 0.007 | 0.340 |
| | DAWM | 0.009 | 0.021 | 0.023 | 0.860 |
| | T2L | 0.010 | 0.020 | 0.022 | 0.793 |
| DVF | NAWM | 0.527 | 0.472 | 0.707 | 0.446 |
| | DAWM | 4.114 | 8.987 | 9.884 | 0.827 |
| | T2L | 3.934 | 16.278 | 16.746 | 0.945 |

**Table 4**
Absolute clinical disability score development of CIS patients over the study period. Whereas the EDSS was measured at baseline and at the end of the study period, the MSFC was determined at all four time points.

| | Baseline<br>*Min … Max*<br>*Median* (IQR) | 3 months | 6 months | 12 months |
|---|---|---|---|---|
| EDSS | 1.0 … 2.5<br>1.5 (0.5) | – | – | 0.0 … 2.0<br>1.5 (0.8) |
| MSFC | 0.3 … 1.3<br>0.7 (0.6) | 0.4 … 1.5<br>0.8 (0.5) | 0.7 … 1.8<br>1.0 (0.4) | 0.4 … 1.7<br>1.0 (0.3) |

### *4.3. Myelin deficiency involved perilesional diffusely abnormal white matter in early MS converters*

As a matter of fact MS converters within this cohort had on average lower values of MWF and a higher DVF even in DAWM what may support the assumption of in vivo detectable non-focal spread of demyelinating activity. In this respect, the occurrence of an isolated neurological symptom may be a consequence of a time-variant occurrence of lesions in eloquent areas. Assuming different degrees of disease progress at onset in individual patients the extensiveness of in vivo measurable myelin deficiency at the first diagnostic imaging may be tremendously different.

Nevertheless, this study accentuates the importance of WM lesion demyelination in early MS. In particular DVF in WM lesions here was sensitive against inflammatory activity of patients in a repeated measure analysis. Hence, there is evidence to suggest valuable additional information hidden within WM lesions. We presume substantial variation of myelination within this hereby cumulatively analyzed lesion VOI. However, novel post-processing techniques are necessary to comprehend such individual lesion myelination differences.

### *4.4. Clinical multiple sclerosis scores did not correlate with regional myelin deficiency*

The clinical scores (*EDSS, MSFC*) available in this cohort in the first year after diagnosis did not correlate with the myelin imaging parameters. This may be a result of this rather small cohort or more likely due to our very early recruitment. Further limiting, the EDSS was only collected at baseline and month 12, missing the in between time points when subjects may have converted to definite MS. This finding is contrasted by our previous results where patients with long-standing CIS in fact revealed a correlation with the EDSS (Kitzler et al., 2012). However, other quantitative but limited myelin-specific techniques like MTI have also revealed a correlation between MTR values in WM lesions and clinical disability but in established MS (Amann et al., 2015). Alternatively the non-significant correlation between the tested novel markers and the clinical scores and unanticipated direction of their association may be attributed to functional compensation in CIS and early stages of MS regardless of tissue destruction comparable with findings of other groups (Uher et al., 2014).

Since the early MS course is predominantly determined by inflammatory demyelination (Brück and Stadelmann, 2003) one of the major restrictions of conventional MRI is its limitation to specifically reflect this direct disease effect. Other more specialized imaging approaches, e.g., the location of WM lesions (Giorgio et al., 2013) or immunological markers, e.g. the levels of serum interleukin-8 (Rossi et al., 2015) have therefore been probed for their correlation to MS development. Hence, our results supplement studies of regarding the

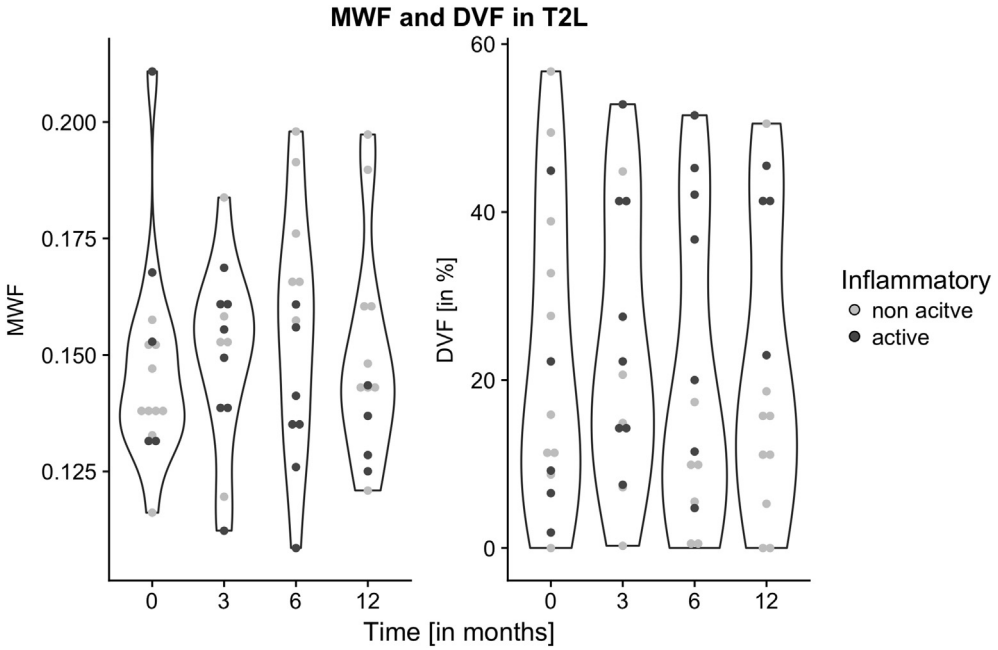


**Fig. 4.** Violin plots for MWF and DVF in T2L of the CIS group. At each time point, the patients are discriminable by the presence of Gadolinium enhancement in data point filling. Note the evolving waist in DVF depicting a higher probability of high DVF values in patients with inflammatory activity.

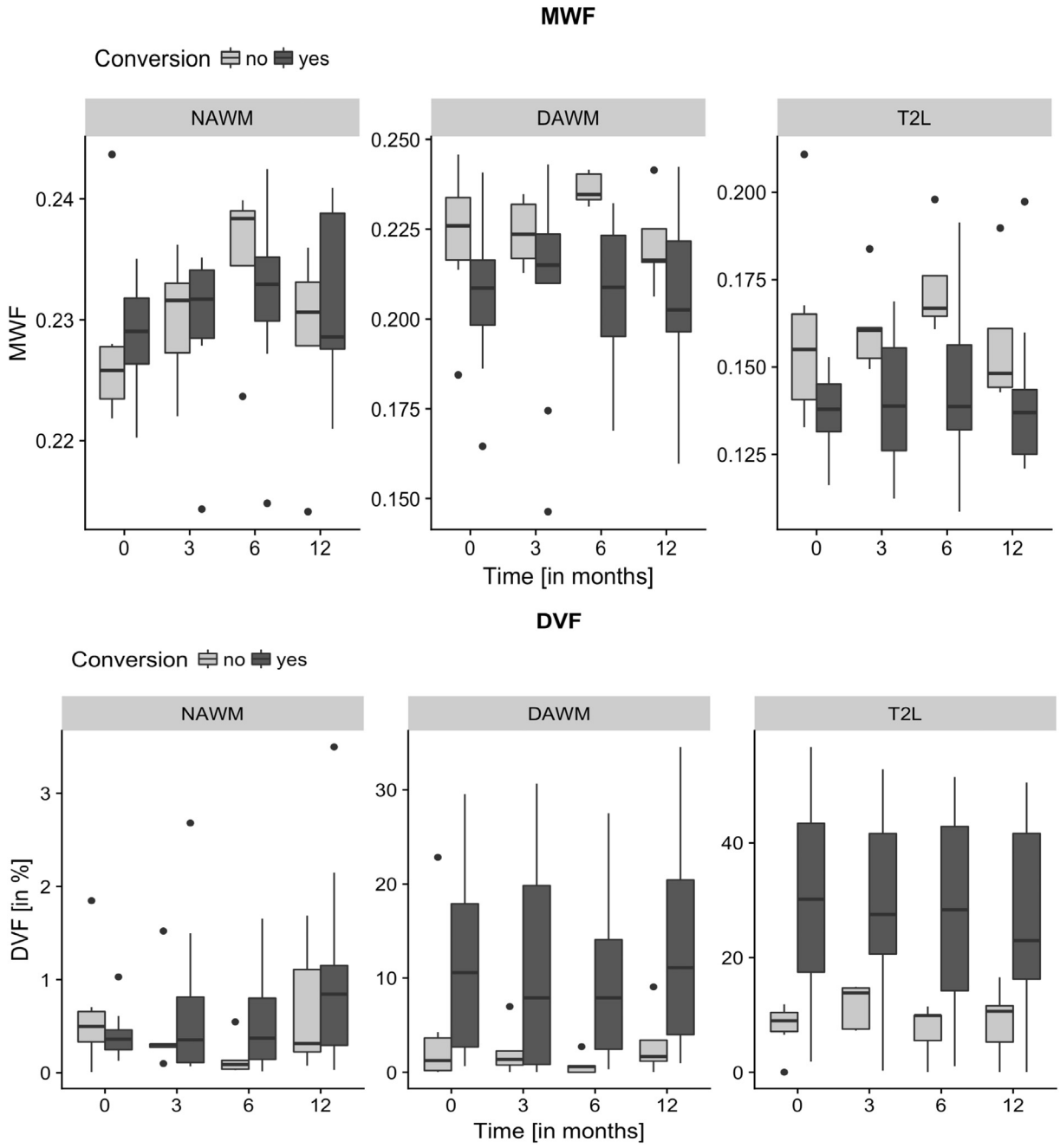


**Fig. 5.** Comparative parallel plots of both MWF and DVF of the CIS subgroups that either converted to clinically definite MS or not at the end of the study period. This revealed an obvious association of a higher variation of DVF in particular in T2 lesions.

**Table 5**
Mean differences between MS-converters and non-converters (as estimated across time points by a linear mixed model) are given for the different WM regions in CIS and their associated *p*-values for MWF and DVF. In addition the mean differences for GM and WM volumes were tested. Significance level was marked with * $p < 0.05$.

| | MWF | DVF [%] | Volume [$mm^3$] |
|---|---|---|---|
| GM | – | – | −13,092.39 ($p = 0.463$) |
| Total WM | – | – | 17,604.49 ($p = 0.343$) |
| NAWM | 0.001 ($p = 0.919$) | −0.025 ($p = 0.996$) | – |
| DAWM | −0.013 ($p = 0.144$) | 5.759 ($p = 0.267$) | – |
| T2L | −0.018 ($p = 0.051$) | 18.354 ($p = 0.002$)* | – |

early prediction of CIS conversion to definite MS.

## 5. Conclusion

The clinical diagnostic exploratory process of both CIS and MS has recently been exceedingly subsidized by MRI criteria. Applying the current revised McDonald criteria for MS based on conventional MRI (Polman et al., 2011), more simplified criteria were proposed before for patients with CIS than before (Swanton et al., 2007). Noteworthy, the definition of patients at risk for developing definite MS when presenting with isolated symptoms remains a relevant clinical challenge not reflected by current diagnostic criteria. Quantitative MRI techniques that are more specific against MS histopathology reveal earliest disease related tissue changes not detectable by conventional MRI. However, their impact on the diagnostic accuracy yet has to be addressed

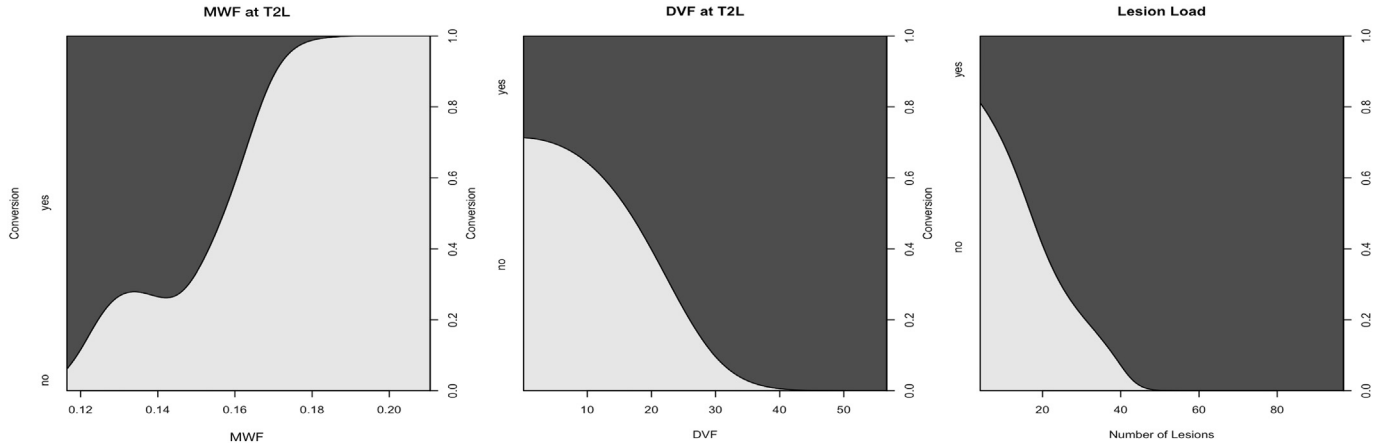


**Fig. 6.** Conditional density plots of myelin measures of MWF and DVF in WM lesions (T2L) and WM lesion load (number of lesions). These plots show a smoothed estimate of how the proportion of converters depends on a metric predictor variable.

irrespectively.

In this regard this is the first report of a CIS patient cohort that was followed up since onset by means of a myelin imaging technique. The whole-brain 3D spatially resolved acquisition and standard brain space group comparison facilitated accurate regional exploration of MS specific myelin changes. This approach may provide future prospects of advanced quantitative MRI diagnostics of MS development. Such objective quantitative evidence of disease activity has recently been incorporated into the novel concept of *no evidence of disease activity* (NEDA) in form of new lesions, lesion volume change over time and brain volume loss (Stangel et al., 2015).

Future studies are needed to investigate in vivo myelin deficiency in established and progressive MS to comprehend its dynamic and variation. With regard to CIS the correlation between spatial distributions of individual lesion myelin loss, clinical disability and disease conversion risk accordingly will give specific insights into early MS myelination dynamics and its impact on brain functional deficiency. Clinical studies in contrast may eventually use myelin imaging in CIS to determine if appropriate treatment may slow down the chance of MS conversion.

## Acknowledgement

We thank all patients and their families for their generous agreement to the study in times of tumbling diagnoses, their support and effort of time. A special gratitude is given to Janka Russig and Kerstin Liesk for their assistance in acquiring the imaging data.

This work was supported by a NOVARTIS research grant (MFTY720A_FVTW028). We thank NOVARTIS Pharma GmbH, Germany for encouragement and sponsorship.

## References

Amann, M., Papadopoulou, A., Andelova, M., Magon, S., Mueller-Lenke, N., Naegelin, Y., Stippich, C., Radue, E.W., Bieri, O., Kappos, L., Sprenger, T., 2015. Magnetization transfer ratio in lesions rather than normal-appearing brain relates to disability in patients with multiple sclerosis. J. Neurol. 262, 1909–1917.

Ashburner, J., Friston, K.J., 2005. Unified segmentation. NeuroImage 26, 839–851.

Brück, W., Stadelmann, C., 2003. Inflammation and degeneration in multiple sclerosis. Neurol. Sci. Suppl. 5, S265–S267.

Charil, A., Filippi, M., 2007. Inflammatory demyelination and neurodegeneration in early multiple sclerosis. J. Neurol. Sci. 259, 7–15.

Cicarelli, E.C., 2000. Medicine in the past millennium. N. Engl. J. Med. 342, 1365.

Cutter, G.R., Baier, M.L., Rudick, R.A., Cookfair, D.L., Fischer, J.S., Petkau, J., Syndulko, K., Weinshenker, B.G., Antel, J.P., Confavreux, C., Ellison, G.W., Lublin, F., Miller, A.E., Rao, S.M., Reingold, S., Thompson, A., Willoughby, E., 1999. Development of a multiple sclerosis functional composite as a clinical trial outcome measure. Brain 122, 871–882.

Deoni, S.C.L., Rutt, B.K., Jones, D.K., 2008. Investigating exchange and multicomponent relaxation in fully-balanced steady-state free precession imaging. J. Magn. Reson. Imaging 27, 1421–1429.

Fazekas, F., Barkhof, F., Filippi, M., Grossman, R., Li, D., McDonald, W., McFarland, H., Paty, D., Simon, J., Wolinsky, J., 1999. The contribution of magnetic resonance imaging to the diagnosis of multiple sclerosis. Neurology 53 (448–448).

Fisniku, L.K., Brex, P.A., Altmann, D.R., Miszkiel, K.A., Benton, C.E., Lanyon, R., Thompson, A.J., Miller, D.H., 2008. Disability and T2 MRI lesions: a 20-year follow-up of patients with relapse onset of multiple sclerosis. Brain 131, 808–817.

Giorgio, A., Battaglini, M., Rocca, M.A., De Leucio, A., Absinta, M., van Schijndel, R., Rovira, A., Tintore, M., Chard, D., Ciccarelli, O., Enzinger, C., Gasperini, C., Frederiksen, J., Filippi, M., Barkhof, F., De Stefano, N., Group, M.S., 2013. Location of brain lesions predicts conversion of clinically isolated syndromes to multiple sclerosis. Neurology 80, 234–241.

Greve, D.N., Fischl, B., 2009. Accurate and robust brain image alignment using boundary-based registration. NeuroImage 48, 63–72.

Jenkinson, M., Smith, S., 2001. A global optimisation method for robust affine registration of brain images. Med. Image Anal. 5, 143–156.

Jenkinson, M., Bannister, P., Brady, M., Smith, S., 2002. Improved optimization for the robust and accurate linear registration and motion correction of brain images. NeuroImage 17, 825–841.

Jenkinson, M., Pechaud, M., Smith, S., 2005. BET2: MR-based Estimation of Brain, Skull and Scalp Surfaces. Eleventh Annual Meeting of the Organization for Human Brain Mapping.

Kitzler, H.H., Su, J., Zeineh, M., Harper-Little, C., Leung, A., Kremenchutzky, M., Deoni, S.C., Rutt, B.K., 2012. Deficient MWF mapping in multiple sclerosis using 3D whole-brain multi-component relaxation MRI. NeuroImage 59, 2670–2677.

Korteweg, T., Uitdehaag, B.M., Knol, D.L., Smithuis, R.H., Algra, P.R., de Vries, C., Poppe, P.A., van Waesberghe, J.H., Bergers, E., Lycklama a Nijeholt, G.J., Polman, C.H., Barkhof, F., 2007. Interobserver agreement on the radiological criteria of the international panel on the diagnosis of multiple sclerosis. Eur. Radiol. 17, 67–71.

Krupp, L.B., Banwell, B., Tenembaum, S., International Pediatric, M.S.S.G, 2007. Consensus definitions proposed for pediatric multiple sclerosis and related disorders. Neurology 68, S7–12.

Krupp, L.B., Tardieu, M., Amato, M.P., Banwell, B., Chitnis, T., Dale, R.C., Ghezzi, A., Hintzen, R., Kornberg, A., Pohl, D., Rostasy, K., Tenembaum, S., Wassmer, E., International Pediatric Multiple Sclerosis Study, G, 2013. International Pediatric Multiple Sclerosis Study Group criteria for pediatric multiple sclerosis and immune-mediated central nervous system demyelinating disorders: revisions to the 2007 definitions. Mult. Scler. 19, 1261–1267.

Kuhle, J., Disanto, G., Dobson, R., Adiutori, R., Bianchi, L., Topping, J., Bestwick, J.P., Meier, U.C., Marta, M., Dalla Costa, G., Runia, T., Evdoshenko, E., Lazareva, N., Thouvenot, E., et al., 2015. Conversion from clinically isolated syndrome to multiple sclerosis: a large multicentre study. Mult. Scler. 21, 1013–1024.

Kurtzke, J.F., 1983. Rating neurologic impairment in multiple sclerosis: an expanded disability status scale (EDSS). Neurology 33 (11), 1444–1452 (Nov).

Laule, C., Vavasour, I., Kolind, S., Li, D.B., Traboulsee, T., Moore, G.R.W., MacKay, A., 2007. Magnetic resonance imaging of myelin. Neurotherapeutics 4, 460–484.

Miller, D., Barkhof, F., Montalban, X., Thompson, A., Filippi, M., 2005a. Clinically isolated syndromes suggestive of multiple sclerosis, part 1: natural history, pathogenesis, diagnosis, and prognosis. Lancet Neurol. 4, 281–288.

Miller, D., Barkhof, F., Montalban, X., Thompson, A., Filippi, M., 2005b. Clinically isolated syndromes suggestive of multiple sclerosis, part 2: non-conventional MRI, recovery processes, and management. Lancet Neurol. 4, 341–348.

Miller, D.H., Weinshenker, B.G., Filippi, M., Banwell, B.L., Cohen, J.A., Freedman, M.S., Galetta, S.L., Hutchinson, M., Johnson, R.T., Kappos, L., Kira, J., Lublin, F.D., McFarland, H.F., Montalban, X., Panitch, H., Richert, J.R., Reingold, S.C., Polman, C.H., 2008. Differential diagnosis of suspected multiple sclerosis: a consensus approach. Mult. Scler. 14, 1157–1174.

Nielsen, J.M., Pohl, C., Polman, C.H., Barkhof, F., Freedman, M.S., Edan, G., Miller, D.H., Bauer, L., Sandbrink, R., Kappos, L., Uitdehaag, B.M., 2009. MRI characteristics are predictive for CDMS in monofocal, but not in multifocal patients with a clinically isolated syndrome. BMC Neurol. 9, 19.

Polman, C.H., Reingold, S.C., Banwell, B., Clanet, M., Cohen, J.A., Filippi, M., Fujihara, K., Havrdova, E., Hutchinson, M., Kappos, L., Lublin, F.D., Montalban, X., O'Connor, P., Sandberg-Wollheim, M., Thompson, A.J., Waubant, E., Weinshenker, B., Wolinsky, J.S., 2011. Diagnostic criteria for multiple sclerosis: 2010 revisions to the McDonald criteria. Ann. Neurol. 69, 292–302.

Rossi, S., Motta, C., Studer, V., Macchiarulo, G., Germani, G., Finardi, A., Furlan, R., Martino, G., Centonze, D., 2015. Subclinical central inflammation is risk for RIS and CIS conversion to MS. Mult. Scler. 21, 1443–1452.

Smith, S.M., 2002. Fast robust automated brain extraction. Hum. Brain Mapp. 17, 143–155.

Smith, S.M., Jenkinson, M., Woolrich, M.W., Beckmann, C.F., Behrens, T.E.J., Johansen-Berg, H., Bannister, P.R., De Luca, M., Drobnjak, I., Flitney, D.E., Niazy, R.K., Saunders, J., Vickers, J., Zhang, Y., De Stefano, N., Brady, J.M., Matthews, P.M., 2004. Advances in functional and structural MR image analysis and implementation as FSL. NeuroImage 23 (Supplement 1), S208–S219.

Stangel, M., Penner, I.K., Kallmann, B.A., Lukas, C., Kieseier, B.C., 2015. Towards the implementation of 'no evidence of disease activity' in multiple sclerosis treatment: the multiple sclerosis decision model. Ther. Adv. Neurol. Disord. 8, 3–13.

Swanton, J.K., Rovira, A., Tintore, M., Altmann, D.R., Barkhof, F., Filippi, M., Huerga, E., Miszkiel, K.A., Plant, G.T., Polman, C., 2007. MRI criteria for multiple sclerosis in patients presenting with clinically isolated syndromes: a multicentre retrospective study. Lancet Neurol. 6, 677–686.

Tintore, M., Rovira, A., Rio, J., Nos, C., Grive, E., Tellez, N., Pelayo, R., Comabella, M., Sastre-Garriga, J., Montalban, X., 2006. Baseline MRI predicts future attacks and disability in clinically isolated syndromes. Neurology 67, 968–972.

Uher, T., Blahova-Dusankova, J., Horakova, D., Bergsland, N., Tyblova, M., Benedict, R.B., Kalincik, T., Ramasamy, D., Seidl, Z., Hagermeier, J., Vaneckova, M., Krasensky, J., Havrdova, E., Zivadinov, R., 2014. Longitudinal MRI and neuropsychological assessment of patients with clinically isolated syndrome. J. Neurol. 1–10.

Whittall, K.P., MacKay, A.L., Graeb, D.A., Nugent, R.A., Li, D.K., Paty, D.W., 1997. In vivo measurement of T2 distributions and water contents in normal human brain. Magn. Reson. Med. 37, 34–43.

Yushkevich, P.A., Piven, J., Hazlett, H.C., Smith, R.G., Ho, S., Gee, J.C., Gerig, G., 2006. User-guided 3D active contour segmentation of anatomical structures: significantly improved efficiency and reliability. NeuroImage 31, 1116–1128.

Zhang, Y., Brady, M., Smith, S., 2001. Segmentation of brain MR images through a hidden Markov random field model and the expectation-maximization algorithm. IEEE Trans. Med. Imaging 20, 45–57.